Quark magnetar in the three-flavor Nambu–Jona-Lasinio model with vector interactions and a magnetized gluon potential

Peng-Cheng Chu,[1,2,*] Xin Wang,[1,†] Lie-Wen Chen,[1,3,‡] and Mei Huang[2,4,§]

[1]*Department of Physics and Astronomy and Shanghai Key Laboratory for Particle Physics and Cosmology, Shanghai Jiao Tong University, Shanghai 200240, China*

[2]*Institute of High Energy Physics, Chinese Academy of Sciences, Beijing 100049, China*

[3]*Center of Theoretical Nuclear Physics, National Laboratory of Heavy-Ion Accelerator, Lanzhou 730000, China*

[4]*Theoretical Physics Center for Science Facilities, Chinese Academy of Sciences, Beijing 100049, China*

(Received 4 October 2014; published 12 January 2015)

We investigate properties of strange quark matter in the framework of the SU(3) Nambu–Jona-Lasinio model with vector interactions under strong magnetic fields. The effects of vector-isoscalar and vector-isovector interactions on the equation of state of strange quark matter are investigated, and it is found that the equation of state is not sensitive to the vector-isovector interaction; however, a repulsive interaction in the vector-isoscalar channel gives a stiffer equation of state for cold dense quark matter. In the presence of a magnetic field, gluons will be magnetized via quark loops, and the contribution from magnetized gluons to the equation of state is also estimated. The sound velocity square is a quantity to measure the hardness or softness of dense quark matter, and in the Nambu–Jona-Lasinio model without vector interaction at zero magnetic field, the sound velocity square is always less than $1/3$. It is found that a repulsive vector-isoscalar interaction and a positive pressure contribution from magnetized gluons can enhance the sound velocity square, which can even reach 1. To construct quark magnetars under strong magnetic fields, we consider anisotropic pressures and use a density-dependent magnetic field profile to mimic the magnetic field distribution in a quark star. We also analyze the parameter region for the magnitude of vector-isoscalar interaction and the contribution from magnetized gluons in order to produce two-solar-mass quark magnetars.

DOI: 10.1103/PhysRevD.91.023003 PACS numbers: 21.65.Qr, 21.30.Fe, 26.60.Kp, 97.60.Jd

I. INTRODUCTION

Investigating properties of strong interaction matter is one of the main topics of quantum chromodynamics (QCD). It is believed that there will be deconfinement phase transition from hadronic matter to quark-gluon plasma at sufficiently high temperatures and from nuclear matter to quark matter (or color superconductor) at high baryon densities. The hot quark-gluon plasma is expected to be created in heavy ion collisions at the Relativistic Heavy Ion collider (RHIC) and the Large Hadron Collider (LHC). The hot and dense quark matter might be created in heavy ion collisions at FAIR in GSI and the Nuclotron-based Ion Collider Facility (NICA) at JINR, while the cold and dense quark matter may exist in the inner core of compact stars.

In the inner core of compact stars, the baryon density can reach or even be larger than about six times the normal nuclear matter density $n_0 = 0.16$ fm^{-3}, so there might exist "exotic" matter like hyperons [1–3], meson condensations [4–6], and quark matter (normal quark matter or strange quark matter [7,8] and a color superconductor [9,10]). Strange quark matter has been conjectured to be the true ground state of QCD [7,8], and many efforts have been put on investigating the conversion from a neutron star to a quark star that consists of strange quark matter that is made purely by u, d, and s quarks and some leptons like the electron and muon due to charge neutrality and β equilibrium [11–14]. There are also hybrid star conjectures on a transition from the nuclear phase to quark phase at such high baryon density, and several authors have studied the phase transition in a hybrid star [15–23].

The equation of state (EoS) plays a central role in investigating properties of strong interaction matter, which is one of fundamental issues in nuclear physics, astrophysics, and cosmology. On the one hand, the EoS generates unique mass vs radius relations for neutron stars and the ultradense remnants of stellar evolution. On the other hand, the mass-radius relation of compact stars can put strong constraints on the EoS for strong interaction matter at high baryon density and low temperature.

Recently, the two heaviest neutron stars have been measured with high accuracy. One is the radio pulsar J1614-2230 [24] with a mass of $1.97 \pm 0.04 M_\odot$, and the other is J0348+0432 [25] with mass $2.01 \pm 0.04 M_\odot$. Even heavier neutron stars have been discussed in the literature [26,27]. It is suggested that the established existence of

*kyois@sjtu.edu.cn
†xinwang@sjtu.edu.cn
‡lwchen@sjtu.edu.cn
§huangm@mail.ihep.ac.cn

 © 2015 American Physical Society

two-solar-mass neutron stars would prefer a hard EoS based entirely on conventional nuclear degrees of freedom, and many soft equations of state, including hybrid stars containing significant exotic proportions of hyperons, Bose condensates, or quark matter would be ruled out.

However, it has been pointed out that the repulsive vector interaction in the Nambu–Jona-Lasinio (NJL) model can produce a stiff EoS for dense quark matter and thus can generate a two-solar-mass compact star [28,29]. The role of the vector interaction in the QCD vacuum and medium has been discussed in much of the literature [28–46]. The introduction of the vector interaction within the NJL model is necessary to describe vector mesons, and the coupling constant is determined by the vector spectra [30,33]. To describe vector bound states within the NJL model, the vector interaction must be attractive in the spacelike components; thus, it is repulsive in the timelike components, which is relevant for the number density in the mean field [34]. The QCD phase diagram and the critical end point are sensitive to the sign of vector coupling constant as shown in Refs. [38–41].

Furthermore, the presence of an external magnetic field can even harden the equation of state of dense quark matter as shown in Ref. [47]. In recent decades, properties of hot and dense quark matter under strong magnetic fields have attracted lots of interest; especially, in the recent several years, much progress has been made.

Strong magnetic fields with the strength of 10^{18}–10^{20} G [equivalent to $eB \sim (0.1\text{–}1.0\ \mathrm{GeV})^2$] can be generated in the laboratory through noncentral heavy ion collisions [48,49] at the RHIC and the LHC. This offers a unique opportunity to study properties of hot strong-interaction matter under a strong magnetic field. The observation of charge azimuthal correlations at the RHIC and LHC [50,51] might indicate the anomalous chiral magnetic effect [52–54] with local P and CP violation. Conventional chiral symmetry breaking and restoration under external magnetic fields has been investigated for many years. It has been recognized for more than 20 years that the chiral condensate increases with B, which is called magnetic catalysis [55–57], and naturally the chiral symmetry should be restored at a higher T_c with an increasing magnetic field. However, the Lattice group [58–60] has demonstrated that the transition temperature decreases as a function of the external magnetic field, i.e., inverse magnetic catalysis around T_c, which is in contrast to the naive expectation and the majority of previous results. It was shown in Refs. [61,62] that the chirality imbalance can explain the inverse magnetic catalysis. It was suggested that in the presence of an external magnetic field there will be vector condensation in the QCD vacuum [63,64], and the vector condensation was confirmed in Refs. [65,66]. The vector condensation in the neutron star has been discussed in Ref. [67].

Moreover, considerable efforts have also been directed to the study of the effects of intense magnetic fields on various astrophysical phenomena. The presence of strong magnetic fields at the surface of conventional compact stars or neutron stars is 10^9–10^{15} G [68–74], which is a thousand times stronger than ordinary neutron stars. These strongly magnetized objects are called magnetars [74]. By using the scalar virial theorem based on Newtonian gravity [75], it is predicted that the magnetic field in the inner core of neutron stars could reach as high as 10^{18}–10^{20} G. Under such tremendous magnetic fields, the $\mathcal{O}(3)$ rotational symmetry will break, and the pressure anisotropy of the system must be considered [76–79]. To mimic the spatial distribution of the magnetic field strength in magnetars, people have introduced a density-dependent magnetic field profile [80,81].

Many efforts have been taken to investigate the existence of a quark core in neutron stars under a strong magnetic field [47,82–88]. In this work, we will use the SU(3) NJL model with vector interaction to investigate the magnetar, and we will also consider the pressure contribution from polarized gluons under a magnetic field.

It is known that the NJL model only considers the quark contribution to the pressure; therefore, the pressure from the NJL model is smaller than that from lattice calculation at high temperature and zero chemical potential [89,90]. To consider the gluon contribution to the pressure, the Polyakov-loop potential was first introduced in the framework of NJL model in Ref. [91] and then in Ref. [92], where the Polyakov-loop potential is temperature dependent. The Polyakov loop-Nambu-Jona-Lasinio (PNJL) model can fit the equation of state at high temperature very well with lattice QCD results. The extension of the Polyakov-loop potential to finite chemical potential is not trivial. To use the PNJL model to describe neutron stars, the Polyakov potential was modified to have chemical potential dependent in Refs. [93–97]. However, there is still no extension of the Polyakov-loop potential under magnetic field. Therefore, we cannot use the PNJL model for our purpose in this work to investigate quark matter at high baryon density under an external magnetic field; thus, we have to find another way to include the gluon contribution to the pressure at finite chemical potential and at magnetic fields. In this work, we will give an ansatz on the potential from magnetized gluons hinted at from hard thermal/dense loop results.

The paper is organized as follows. In Sec. II, we give a general description of the SU(3) NJL model with vector interaction under a magnetic field with β equilibrium, we make an ansatz of the thermodynamical potential from magnetized gluons, and we derive the equation of state of the strange quark matter with β equilibrium. Our numerical results are shown in Sec. III, and the conclusion and discussion is given in Sec. IV.

II. THREE-FLAVOR NJL MODEL WITH VECTOR INTERACTIONS UNDER A MAGNETIC FIELD

We study properties of three-flavor system with external strong magnetic fields A_μ^{ext} under the β equilibrium condition, which is described by the Lagrangian density

$$\mathcal{L} = \mathcal{L}_q + \mathcal{L}_e - \frac{1}{4}F_{\mu\nu}F^{\mu\nu}, \tag{1}$$

where $\mathcal{L}_q$ and $\mathcal{L}_e$ are the Lagrangian densities for quarks and electrons, respectively. $F_{\mu\nu} = \partial_\mu A_\nu^{\text{ext}} - \partial_\nu A_\mu^{\text{ext}}$ is the strength tensor for external electromagnetic field. The magnetic field B is a static magnetic field along the z direction, and $A_\mu^{\text{ext}} = \delta_{\mu 2} x_1 B$. In this work, we do not consider contributions from the anomalous magnetic moments [98].

The electron Lagrangian density is given as

$$\mathcal{L}_e = \bar{e}[(i\partial_\mu - eA_{\text{ext}}^\mu)\gamma^\mu]e. \tag{2}$$

The Lagrangian density for quarks is described by the gauged $N_f = 3$ NJL model with vector interaction [31,32]

$$\mathcal{L}_q = \bar{\psi}_f[\gamma_\mu(i\partial^\mu - q_f A_{\text{ext}}^\mu) - \hat{m}_c]\psi_f + \mathcal{L}_4 + \mathcal{L}_6, \tag{3}$$

where $\mathcal{L}_4$ indicates four-fermion interaction compatible with QCD symmetries $SU(3)_{\text{color}} \otimes SU(3)_L \otimes SU(3)_R$ and $\mathcal{L}_6$ is the six-point interaction which is required to break the axial $U(1)_A$ symmetry. $\psi = (u, d, s)^T$ represents a quark field with three flavors, $\hat{m}_c = \text{diag}(m_u, m_d, m_s)$ is the current quark mass matrix, and q_f is the quark electric charge. The four-fermion interaction includes scalar, pseudoscalar, vector, and axial-vector channels and takes the form of

$$\mathcal{L}_4 = \mathcal{L}_S + \mathcal{L}_V + \mathcal{L}_{I,V}. \tag{4}$$

The scalar part takes the form of

$$\mathcal{L}_S = G_S \sum_{a=0}^{8}[(\bar{\psi}_f \lambda_a \psi_f)^2 + (\bar{\psi}_f i\gamma_5 \lambda_a \psi_f)^2], \tag{5}$$

and the vector part is given as

$$\mathcal{L}_V = -G_V \sum_{a=0}^{8}[(\bar{\psi}\gamma^\mu \lambda^a \psi)^2 + (\bar{\psi} i\gamma^\mu \gamma_5 \lambda^a \psi)^2], \tag{6}$$

where G_S and G_V are the coupling constants in the scalar and vector channels, respectively. $\lambda_a (a = 1, \ldots, 8)$ λ_a are the Gell–Mann matrices and the generators of the SU(3) flavor groups, and $\lambda_0 = \sqrt{2/3}I$ with I the 3×3 unit matrix. To describe the nonet of scalars, pseudoscalars, vectors, and axial-vectors, a convenient representation is obtained by changing from $\{\lambda_0, \lambda_1, \ldots, \lambda_8\}$ to the set $\{\lambda_0, \lambda_1^\pm, \lambda_3, \lambda_4^\pm, \lambda_6^\pm, \lambda_8\}$ with

$$\lambda_1^\pm = \sqrt{\frac{1}{2}}(\lambda_1 \pm i\lambda_2),$$
$$\lambda_4^\pm = \sqrt{\frac{1}{2}}(\lambda_4 \pm i\lambda_5),$$
$$\lambda_6^\pm = \sqrt{\frac{1}{2}}(\lambda_6 \pm i\lambda_7).$$

Hadrons in the u, d sector exhibit $SU(2)_I$ isospin symmetry. Up and down quarks have isospin $I = 1/2$ and isospin 3-components (I_3) of $1/2$ and $-1/2$, respectively. All other quarks have $I = 0$. For scalars, the coupling constant in the scalar-isoscalar (σ) and pseudoscalar-isovector (π) interactions have to be equal, which is constrained by chiral symmetry. However, the coupling constants for the vector-isoscalar (ω) and vector-isovector (ρ) interactions can be separately invariant and thus can be chosen independently. The ratio of the coupling constants of the vector-isosinglet channel ω and vector-isovector channel ρ to nucleons is empirically given by $g_{\omega QQ}/g_{\rho QQ} \simeq 3$ in the chirally broken phase, and $g_{\omega QQ}/g_{\rho QQ} = 1$ in the chiral symmetric phase [39,98,99]. To distinguish the isoscalar and isovector for vectors, we introduce an extra term for the vector-isovector channel with the form of

$$\mathcal{L}_{IV} = -G_{IV}[(\bar{\psi}\gamma^\mu \vec{\tau}\psi)^2 + (\bar{\psi}\gamma_5\gamma^\mu \vec{\tau}\psi)^2]. \tag{7}$$

The coupling constant for vector-isoscalar $G_V^\omega = G_V$, and the coupling constant for vector-isovector $G_V^\rho = G_V + G_{IV}$. In this work, we will investigate the role of the vector-isovector interaction on the equation of state; therefore, in our numerical calculations, we choose G_{IV} as a free parameter.

The six-fermion interaction $\mathcal{L}_6$, i.e., the 't Hooft term, takes the form of

$$\mathcal{L}_{\text{det}} = -K\{\det{}_f[\bar{\psi}_f(1+\gamma_5)\psi_f] + \det{}_f[\bar{\psi}_f(1-\gamma_5)\psi_f]\}, \tag{8}$$

which is to break the $U(1)_A$ symmetry.

A. Pressure from quark contribution

The equation of state is the most important aspect for physicists to acquire the properties of quark matter. To get the pressure and energy density of quark matter, we should first derive the thermodynamical potential Ω_f. In the procedure, we can calculate the thermodynamical quantities by using finite-temperature field theory. In the mean-field approximation, the Lagrangian density for quark part is

$$\mathcal{L}_M = \bar{\psi}_f[\gamma_\mu(i\partial^\mu - q_f A^\mu_{\rm ext}) - \hat{M} - 2G_{IV}\gamma_0\tau_{3f}n_f]\psi_f - 2G_S(\sigma_u^2+\sigma_d^2+\sigma_s^2) + 4K\sigma_u\sigma_d\sigma_s - 4G_V\gamma_0\hat{n} + 2G_V(n_u^2+n_d^2+n_s^2) + G_{IV}(n_u-n_d)^2, \quad (9)$$

where

$$\hat{n} = \begin{pmatrix} n_u & 0 & 0 \\ 0 & n_d & 0 \\ 0 & 0 & n_s \end{pmatrix}$$

and

$$\hat{M} = \begin{pmatrix} M_u & 0 & 0 \\ 0 & M_d & 0 \\ 0 & 0 & M_s \end{pmatrix}.$$

The quark mass is determined by the gap equation of

$$M_i = m_i - 4G_S\sigma_i + 2K\sigma_j\sigma_k, \quad (10)$$

with (i,j,k) being any permutation of (u,d,s), and the chiral condensate is given as

$$\sigma_f = \langle\bar{\psi}_f\psi_f\rangle = -i\int\frac{d^4p}{(2\pi)^4}\mathrm{tr}\frac{1}{(\not{p} - M_f + i\epsilon)}. \quad (11)$$

After introducing Landau quantization and several steps of finite-temperature field theory calculations, we can get the thermodynamical potential Ω_q of quark matter under magnetic fields, and the pressure density $p_q = -\Omega_q$ and takes the form of

$$p_q = -2G_S(\sigma_u^2+\sigma_d^2+\sigma_s^2) + 4K\sigma_u\sigma_d\sigma_s + 2G_V(n_u^2+n_d^2+n_s^2) + G_{IV}(n_u-n_d)^2 + (\Omega^u_{ln} + \Omega^d_{ln} + \Omega^s_{ln}), \quad (12)$$

with the logarithmic contribution

$$\Omega^f_{\rm ln} = -i\int\frac{d^4p}{(2\pi)^4}\mathrm{tr}\ln\left\{\frac{1}{T}[\not{p} - \hat{M}_f + \gamma_0\tilde{\mu}_f]\right\}; \quad (13)$$

here,

$$\tilde{\mu}_f = \mu_f - 4G_V n_f - 2G_{IV}\tau_{3f}(n_u - n_d), \quad (14)$$

where μ_f is the chemical potential for each flavor of quarks and τ_{3f} is the isospin quantum number for quarks: $\tau_{3u} = 1$, $\tau_{3d} = -1$, and $\tau_{3s} = 0$.

Following Ref. [47], one can get the condensates and pressure for quarks. The logarithmic contribution to the thermodynamical potential is given by

$$\Omega^f_{\rm ln} = \Omega^{f,\rm vac}_{\rm ln} + \Omega^{f,\rm mag}_{\rm ln} + \Omega^{f,\rm med}_{\rm ln}. \quad (15)$$

The first term is the vacuum contribution

$$\Omega^{f,\rm vac}_{\rm ln} = -\frac{N_c}{8\pi^2}\left\{M_f^4\ln\left[\frac{\Lambda+\epsilon_\Lambda}{M_f}\right] - \epsilon_\Lambda\Lambda(\Lambda^2+\epsilon_\Lambda^2)\right\}, \quad (16)$$

with $\epsilon_\Lambda^2 = \Lambda^2 + M_f^2$ and Λ the noncovariant cutoff. The magnetic field contribution takes the form of

$$\Omega^{f,\rm mag}_{\rm ln} = \frac{N_c}{2\pi^2}(|q_f|B)^2\left[\frac{x_f^2}{4} + \zeta'(-1,x_f) - \frac{1}{2}(x_f^2 - x_f)\ln(x_f)\right], \quad (17)$$

where $\zeta(z,x)$ is the Riemann–Hurwitz function and

$$\zeta'(-1,x_f) = d\zeta(z,x)/dz|_{z=-1}, \quad (18)$$

with $x_f = \frac{M_f^2}{2|q_f|B}$. The medium contribution reads

$$\Omega^{f,\rm med}_{\rm ln} = \sum_{k=0}^{k_{f\,\max}}\alpha_k\frac{(|q_f|BN_c)}{4\pi^2}\left\{\tilde{\mu}_f\sqrt{\tilde{\mu}_f^2 - s_f(k,B)^2} - s_f(k,B)^2\ln\left[\frac{\tilde{\mu}_f + \sqrt{\tilde{\mu}_f^2 - s_f(k,B)^2}}{s_f(k,B)}\right]\right\}, \quad (19)$$

where

$$s_f(k,B) = \sqrt{M^2 + 2|q_f|Bk}, \quad (20)$$

and

$$k_{f\,\max} = \frac{\tilde{\mu}_f^2 - M^2}{2|q_f|B} = \frac{p_{f,F}^2}{2|q_f|B} \quad (21)$$

is the upper Landau level with $\alpha_k = 2 - \delta_{k0}$.

Then, we can also give the condensates for each flavor of quarks:

$$\sigma_f = \sigma_f^{\rm vac} + \sigma_f^{\rm mag} + \sigma_f^{\rm med} \quad (22)$$

with

$$\sigma_f^{\rm vac} = -\frac{M_f N_c}{2\pi^2}\left\{\Lambda\sqrt{\Lambda^2+M_f^2} - \frac{M_f^2}{2}\ln\left[\frac{(\Lambda+\sqrt{\Lambda^2+M_f^2})^2}{(M_f^2)}\right]\right\}, \quad (23)$$

$$\sigma_f^{\mathrm{mag}} = -\frac{M_f N_c}{2\pi^2}(|q_f|B)\left\{\ln[\Gamma(x_f)] - \frac{1}{2}\ln(2\pi) + \frac{\ln(x_f)}{2} - x_f \ln(x_f)\right\}, \quad (24)$$

$$\sigma_f^{\mathrm{med}} = \sum_{k=0}^{k_{f\,\max}} \alpha_k \frac{M_f |q_f| B N_c}{\pi^2} \times \left\{\ln\left[\frac{\tilde{\mu}_f + \sqrt{\tilde{\mu}_f^2 - s_f(k,B)^2}}{s_f(k,B)}\right]\right\}. \quad (25)$$

B. Pressure from leptons

For strange quark matter (SQM), we assume it is neutrino free and composed of u, d, and s quarks and e^- in β equilibrium with electric charge neutrality. The weak β-equilibrium condition can then be expressed as

$$\mu_u + \mu_e = \mu_d = \mu_s, \quad (26)$$

where μ_i ($i = u$, d, s, and e^-) is the chemical potential of the particles in SQM. Furthermore, the electric charge neutrality condition can be written as

$$\frac{2}{3}n_u = \frac{1}{3}n_d + \frac{1}{3}n_s + n_e, \quad (27)$$

where

$$n_f = \sum_{k=0}^{k_f,\max} \alpha_k \frac{|q_f| B N_c}{2\pi^2} k_{F,f} \quad (28)$$

is the number density for each flavor of quarks with $k_{F,f} = \sqrt{\tilde{\mu}_f^2 - s_f(k,B)^2}$ and

$$n_l = \sum_{k=0}^{k_l,\max} \alpha_k \frac{|q_l| B}{2\pi^2} k_{F,l} \quad (29)$$

is the number density of electrons.

We can also write the leptonic contribution to the pressure density, which takes the form of

$$p_l = \sum_{k=0}^{k_{l\,\max}} \alpha_k \frac{(|q_l| B N_c)}{4\pi^2}\left\{\mu_l\sqrt{\mu_l^2 - s_l(k,B)^2} - s_l(k,B)^2 \ln\left[\frac{\mu_l + \sqrt{\mu_l^2 - s_l(k,B)^2}}{s_l(k,B)}\right]\right\}. \quad (30)$$

C. Pressure from magnetized gluon potential

It is well known that the NJL model only considers the quark contribution to the pressure, which is smaller than that from lattice calculation at high temperature and zero chemical potential [89,90]. In the presence of a strong magnetic field, not only are quarks polarized along the direction of B, but also gluons will be polarized via the quark loop. There are still few calculations of pressure contributed from magnetized gluon degrees of freedom at zero temperature and finite chemical potential [60,100].

To consider the gluon contribution to the pressure, on the one hand, the Polyakov-loop potential was introduced in the framework of NJL model in Refs. [91,92], in which the Polyakov-loop potential is temperature dependent. The PNJL model can fit the equation of state at high temperature very well with lattice QCD results. However, to extend the Polyakov-loop potential to finite chemical potential and strong magnetic field is nontrivial, although a modified version of the Polyakov potential at finite chemical potential has been proposed in Refs. [93–97]. For our purpose in this work, to describe the magnetar, we cannot use the PNJL model, but we can estimate the gluon contribution to the pressure at finite chemical potential and with magnetic fields from hard-thermal/dense-loop results. At high temperature and zero chemical potential with zero magnetic field, the gluon contribution to the pressure in the PNJL model should merge with hard-thermal-loop result.

Much effort has been given to the perturbation theory (PT) of hard-thermal-loop (HTL) or hard-dense-loop calculation on the equation of state of strong-interaction matter at high temperature and density [101–113]. At high temperature, recent progress up to three-loop HTL calculations [112] shows that the pressure density, energy density, and other thermodynamical properties are in good agreement with available lattice data for temperatures above approximately 300 MeV. The EoS of cold quark matter is accessible through perturbative QCD at high densities and has been determined to order α_s^2 in the strong coupling constant [110].

The pressure density for the ideal gas of quarks and gluons has the form of

$$p^{SB} = p_q^{SB} + p_g^{SB}, \quad (31)$$

$$p_q^{SB} = N_c N_f\left(\frac{7\pi^2 T^4}{180} + \frac{\mu^2 T^2}{6} + \frac{\mu^4}{12\pi^2}\right), \quad (32)$$

$$p_g^{SB} = (N_c^2 - 1)\frac{\pi^2 T^4}{90}. \quad (33)$$

It is noticed that the pressure density for the ideal gas of gluons is only temperature dependent and with no chemical potential dependent. Switching on coupling between quarks and gluons, the gluons will get screening mass

$$m_g^2 = \frac{1}{6}\left[\left(N_c + \frac{1}{2}N_f\right)T^2 + \frac{3}{2\pi^2}\sum_f \mu_f^2\right]g_{\rm eff}^2, \quad (34)$$

and the perturbation theory at one loop gives the pressure density of gluons as

$$p_g^{\rm PT} = p_g^{SB} - N_g\frac{g_{\rm eff}^2}{32}\left[\frac{5}{9}T^4 + \frac{2}{\pi^2}\mu^2T^2 + \frac{1}{\pi^4}\mu^4\right], \quad (35)$$

and the gluon pressure becomes chemical potential dependent via the quark loop, although the coefficient in front of μ^4 is only $1/54$ of that of T^4.

Under the strong magnetic field, a massive resonance $\sim g\sqrt{eB}$ is excited in the longitudinal $(1+1)$ component of the gluon propagator under strong magnetic fields [114]. The corresponding *Debye mass* of the longitudinal gluon fields $A_\parallel$ has the screening mass

$$m_g^2(eB) = \sum_f |q_f|\frac{g_{\rm eff}^2}{4\pi^2}|eB|, \quad (36)$$

at zero temperature and density. One can guess that at nonzero temperature and density the longitudinal gluon fields take the screening mass of

$$m_g^2(T,\mu,eB) = g^2(aT^2 + b\mu^2 + ceB), \quad (37)$$

where a, b, and c are constants. Taking into account the transverse gluons, the pressure density from magnetized gluons can be estimated as

$$p_g(T,\mu;eB) = a_0\mu^2eB + b_0\mu^4 + c_0T^2eB + d_0\mu^2T^2 + e_0T^4, \quad (38)$$

with a_0, b_0, c_0, d_0, and e_0 being free parameters. At zero temperature,

$$p_g(T=0,\mu;eB) = a_0\mu^2eB + b_0\mu^4. \quad (39)$$

Furthermore, for the screening mass of gluons, considering the coefficients in front of eB is almost the same magnitude as that of μ^2, and we neglect the anisotropy pressure density caused by the magnetic field with magnitude $eB < 10^{19}$ G; for simplicity, in this work, we use the ansatz of the pressure density of magnetized gluons

$$p_g(T=0,\mu;eB) = a_0(\mu^2eB + \mu^4) \quad (40)$$

for our numerical calculations. If we directly extend the perturbative gluon pressure, Eq. (35), to the nonperturbative region, the gluon pressure density at zero temperature and finite density should be negative. However, in the moderate baryon density region, the nonperturbative feature of gluons should still play an important role as shown in Refs. [115,116]. The system in the moderate baryon density can be regarded as compositions of quasiquarks described by NJL model and quasigluons. To compensate the quasiquark contribution to the pressure in the NJL model, the quasigluon contribution to the pressure should be also positive. In our numerical calculation, we will take $a_0 > 0$ for the physical case, but we will also take $a_0 < 0$ for reference.

D. Total pressure of SQM with β equilibrium under a magnetic field

Under strong magnetic fields, the $\mathcal{O}(3)$ rotational symmetry in SQM is broken, and the pressure for SQM might become anisotropic; i.e., the longitudinal pressure $P_\parallel$, which is parallel to the magnetic field orientation, is different from the transverse pressure $P_\perp$, which is perpendicular to the orientation of magnetic field. The analytic forms for longitudinal and transverse pressure densities of the system are given by [76]

$$p_\parallel = p - \frac{1}{2}B^2, \quad (41)$$

$$p_\perp = p + \frac{1}{2}B^2 - MB, \quad (42)$$

where we have defined

$$p = p_q + p_l + p_g - p_0, \quad (43)$$

with $p_0 = -\Omega_0 = -\Omega(T=0,\mu=0,B=0)$ the vacuum pressure density, which ensures $p=0$ in the vacuum. M is the system magnetization and takes the form of

$$M = -\partial\Omega/\partial B = \sum_{i=u,d,s,l,g} M_i. \quad (44)$$

The energy density for SQM at zero temperature is given by

$$\epsilon = -p + \sum_{i=u,d,s,l}\mu_i n_i + \frac{1}{2}B^2. \quad (45)$$

One can find that the longitudinal pressure density $p_\parallel$ satisfies the Hugenholtz–Van Hove theorem [88,117], while the transverse pressure density $p_\perp$ does not because of the extra contributions from the magnetic field. We can see that the magnetic energy density term $B^2/2$ contributes oppositely to the longitudinal and transverse pressures under magnetic fields, which will lead to a tremendous pressure anisotropy when the magnetic field is very strong.

III. NUMERICAL RESULTS AND CONCLUSIONS

For our numerical calculations, following Ref. [47], the set of parameters we used is $\Lambda = 631.4$ MeV,

$m_u = m_d = 5.5$ MeV, $m_s = 135.7$ MeV, $G\Lambda^2 = 1.835$, and $K\Lambda^5 = 9.29$.

A. Effect of vector-isovector interaction and vector-isoscalar interaction under a magnetic field

First, we analyze the effect of vector-isovector and vector-isoscalar interactions on the equation of state of strange quark matter, Eq. (12), under zero magnetic field $B = 0$. For zero magnetic field, there is no anisotropy in the system, and the longitudinal pressure density is equal to the transverse pressure density, i.e., $p_{\|} = p_{\perp} = p(B = 0)$.

In Fig. 1, we show the pressure density of SQM as a function of energy density for three cases: 1) $G_V = G_{IV} = 0$, 2) $G_V = 0.8G_S, G_{IV} = 0$, and 3) $G_V = G_{IV} = 0.8G_S$. Comparing cases 1 and 2, one can find that the repulsive vector-isoscalar interaction G_V gives a stiffer equation of state. However, comparing cases 2 and 3, it is observed that the equation of states for these two cases are almost the same, which indicates that the vector-isovector interaction does not affect the equation of state too much in SQM. One can find from Eq. (12) that the contribution from the vector-isovector interaction is mainly dependent on the u-d quark isospin asymmetry $(n_u - n_d)$ and the coupling constant G_{IV}. Since the isospin asymmetry in SQM is small, the vector-isovector interaction is very tiny with the parameter set $G_V = G_{IV} = 0.8G_S$.

It can be understood as the repulsive vector-isoscalar interaction shifts the chemical potential to a larger value, which makes the equation of state stiffer. However, the interaction in the vector-isovector channel shifts the isospin chemical potential, and this effect is negligible for the equation of state under β equilibrium. Therefore, in the following numerical calculations, we simply take $G_{IV} = 0$.

Figure 2 shows the chemical potentials for the u, d, and s quarks as functions of the magnetic field B with $G_V = 0$ and $G_V = 0.8G_S$ at fixed baryon number density $n_b = 10n_0$ in SQM. The chemical potential for each flavor with $G_V = 0.8G_S$ is enhanced magnificently comparing the case of $G_V = 0$, which implies that a stiffer EoS can be generated once considering a large vector-isoscalar coupling constant. One can also observe that, for both cases with $G_V = 0$ and $G_V = 0.8G_S$, the chemical potential for quarks keeps a constant below the magnitude of 10^{19} G and decreases with the constant magnetic field above that.

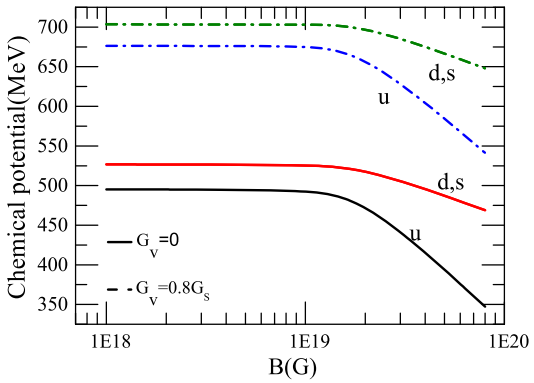

FIG. 2 (color online). Chemical potentials for u, d, and s quarks as functions of a magnetic field with $G_V = 0$ and $G_V = 0.8G_S$ at baryon density $n_b = 10n_0$ in SQM.

Figure 3 shows the constituent mass of the u quark and s quark as functions of baryon density in charge neutral SQM for $B = 0$ and $B = 2 \times 10^{19}$ G with $G_V = 0$ and $G_V = 0.8G_S$, respectively. In the case of zero magnetic field $B = 0$ and $G_V = 0$, the constituent quark mass for the u quark decreases from the vacuum mass almost linearly to 50 MeV in the region of baryon number density below $n_b \simeq 0.35$ fm$^{-3} \simeq 2n_0$ and then slowly decreases with baryon number density. The constituent quark mass for the s quark also drops almost linearly from its vacuum mass to around 475 MeV in the region of baryon number density

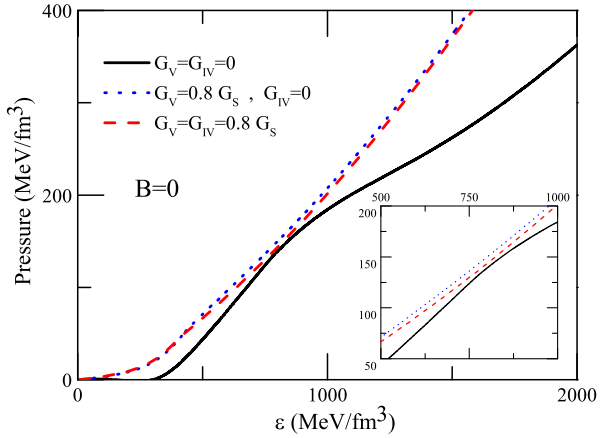

FIG. 1 (color online). The pressure density of SQM as a function of energy density under zero magnetic field with three cases: $G_V = G_{IV} = 0$; $G_V = 0.8G_S$, $G_{IV} = 0$; and $G_V = G_{IV} = 0.8G_S$.

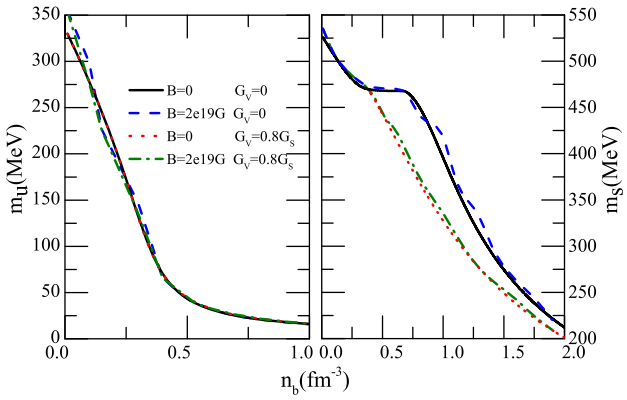

FIG. 3 (color online). Constituent mass for the u quark (left figure) and s quark (right figure) as functions of baryon number density in charge neutral SQM for $B = 0$ and 2×10^{19} G with $G_V = 0$ and $0.8G_s$, respectively.

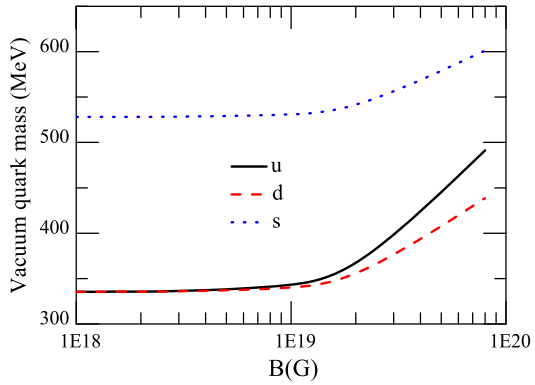

FIG. 4 (color online). Vacuum constituent masses for u, d, and s quarks as functions of the magnetic field in SQM.

below $n_b \simeq 0.35\ \mathrm{fm}^{-3} \simeq 2n_0$ and almost keeps as a constant in the region of $0.35 < n_b < 0.7\ \mathrm{fm}^{-3}$ $(2 < n_b/n_0 < 4)$ and then decreases quickly with baryon number density. This behavior is similar to Fig. 3.9 in Ref. [34]. When the magnetic field is turned on, under the magnitude of $B = 2 \times 10^{19}$ G, only a tiny magnetic catalysis effect can be observed for the u quark and s quark in the low baryon density region, and at a high baryon density region, the magnetic field with magnitude of $B = 2 \times 10^{19}$ G almost has no effect on the constituent quark mass at fixed baryon density. However, it is noticed that the repulsive vector-isoscalar interaction can smooth away the saturation region and make the strange quark mass decrease linearly with the baryon number density.

As shown in Fig. 3, the magnetic field in the magnitude of $B = 2 \times 10^{19}$ G does not essentially affect the constituent quark mass. In Fig. 4, we investigate the vacuum constituent mass of u, d, and s quarks as functions of magnetic field in SQM, and one can find that the masses of three different flavors of quarks do not change so much when the magnetic field is smaller than 10^{19} G, while the u and d quark masses increase drastically when the magnetic field is bigger than 3×10^{19} G, which indicates the magnetic catalysis phenomenon. It should also be noticed that the masses of the d quark and s quark increase more slowly with the magnetic field compared to the u quark mass case.

B. Equation of state, sound velocity, and magnetar mass

As it is accepted, the magnetic field strength in the inner core region of compact stars could be much larger than the magnetic field at the surface; then, a density-dependent magnetic field distribution inside the compact star is usually used to describe this behavior. We use the popular parametrization for the density-dependent magnetic field profile in quark stars (QSs) as in Refs. [81,118–121],

$$B = B_{\mathrm{surf}} + B_0[1 - \exp(-\beta_0(n_b/n_0)^{\gamma})], \qquad (46)$$

where B_{surf} is the magnetic field strength at the surface of compact stars and its value is fixed at $B_{\mathrm{surf}} = 10^{15}$ G in this work; $n_0 = 0.16\ \mathrm{fm}^{-3}$ is the normal nuclear matter density; B_0 is the constant magnetic field, which is a parameter with dimension of B; and β_0 and γ are two dimensionless parameters that control how exactly the magnetic field strength decays from the center to the surface. To reproduce the magnetic field that is weak below the nuclear saturation point while getting stronger at higher density, we take $B_0 = 4 \times 10^{18}$ G, $\beta = 0.003$, and $\gamma = 3$ as the set of parameters in the following calculations, and this magnetic field distribution has already proved to be a gentle magnetic field distribution for SQM inside QSs, which can lead to a small pressure anisotropy and small maximum mass splitting for QSs in a density-dependent quark model [88].

The anisotropic pressure densities in Eqs. (41) and (42) are calculated in cases $B_0 = 0$ and $B_0 = 4 \times 10^{18}$ G with $a_0 = -0.01, 0, 0.01$ and $G_V = 0$, $G_V = 0.4G_S$, $G_V = 0.8G_S$, and $G_V = 1.1G_S$, respectively. We calculate the transverse pressure density as a function of energy density for SQM in Fig. 5, while we calculate the longitudinal pressure case in Fig. 6.

One can see from Fig. 5 that 1) with fixed G_V and fixed a_0 the transverse pressure density for $B_0 = 4 \times 10^{18}$ G is higher than that for $B_0 = 0$; 2) with fixed G_V the positive magnetized gluon pressure density ($a_0 = 0.01$) and the case $B_0 = 4 \times 10^{18}$ G always give the hardest equation of state, while the negative magnetized gluon pressure ($a_0 = -0.01$) and the case $B_0 = 0$ always give the softest equation of state; 3) for the case of negative magnetized gluon pressure ($a_0 = -0.01$) it is found that the equations of state for both $B_0 = 0$ and $B_0 = 4 \times 10^{18}$ G are not sensitive to the value of G_V [however, for the case of positive magnetized gluon pressure ($a_0 = 0.01$), the EoS for both $B_0 = 0$ and $B_0 = 4 \times 10^{18}$ G are very sensitive to the value of G_V]; and 4) when $G_V = 0$ the magnetic field contribution to the equation of state is important, while

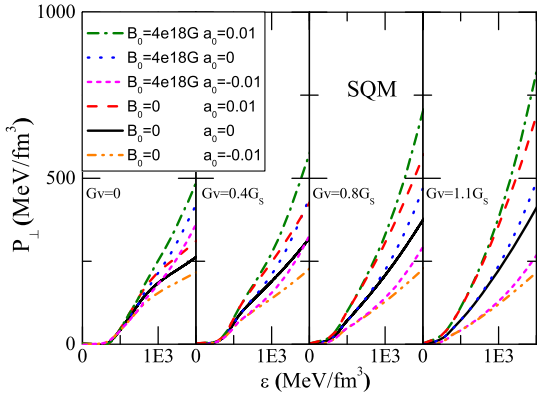

FIG. 5 (color online). Transverse pressure density as a function of energy density for SQM in cases $B_0 = 0$ and $B_0 = 4 \times 10^{18}$ G with $a_0 = 0, 0.01, -0.01$ and $G_V = 0$, $G_V = 0.4G_S$, $G_V = 0.8G_S$, and $G_V = 1.1G_S$, respectively.

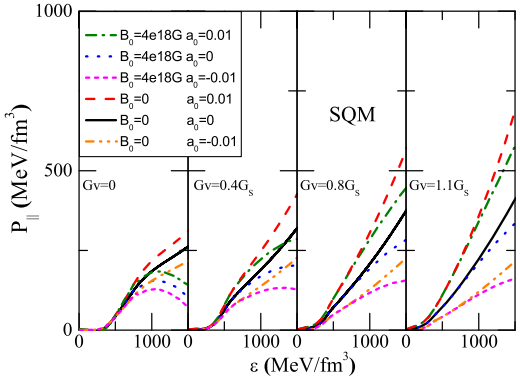

FIG. 6 (color online). Longitudinal pressure density as a function of energy density SQM in cases $B_0 = 0$ and $B_0 = 4 \times 10^{18}$ G with $a_0 = 0, 0.01, -0.01$ and $G_V = 0$, $G_V = 0.4G_S$, $G_V = 0.8G_S$, and $G_V = 1.1G_S$, respectively.

when G_V increases, the contribution from magnetized gluon pressure becomes more and more important to the equation of state.

Shown in Fig. 6 is the longitudinal pressure as a function of energy density of SQM in cases $B_0 = 0$ and $B_0 = 4 \times 10^{18}$ G with $a_0 = 0, 0.01, -0.01$ and $G_V = 0$, $G_V = 0.4G_S$, $G_V = 0.8G_S$, and $G_V = 1.1G_S$, respectively. From this figure, one can find that 1) for $G_V = 0$ and fixed a_0 the longitudinal pressure density for $B_0 = 4 \times 10^{18}$ G is a little smaller than that at $B_0 = 0$, which is opposite of the case of transverse pressure; 2) with fixed G_V the positive magnetized gluon pressure ($a_0 = 0.01$) and the case $B_0 = 0$ always give the hardest equation of state, while the negative magnetized gluon pressure ($a_0 = -0.01$) and the case $B_0 = 4 \times 10^{18}$ G always give the softest equation of state; 3) for the case of negative magnetized gluon pressure ($a_0 = -0.01$) it is found that the equations of state for both $B_0 = 0$ and $B_0 = 4 \times 10^{18}$ G are not sensitive to the value of G_V. However, for the case of positive magnetized gluon pressure ($a_0 = 0.01$), the equations of state for both $B_0 = 0$ and $B_0 = 4 \times 10^{18}$ G are very sensitive to the value of G_V. Compared to Fig 5, we can find that the pressure anisotropy for longitudinal and transverse pressure is small when G_V is as big as $G_V = 0.8G_S$, $G_V = 1.1G_S$ for $a_0 = 0.01$, while the pressure anisotropy gets larger as the decrement of G_V for $a_0 = -0.01$. Compared to the result from Fig. 5, we find the magnetized gluon pressure contribution is more important to stiffen the EoS for SQM than the contribution from magnetic field, and by using this contribution from the magnetized gluon, one can describe a heavy QS (about $2M_\odot$) with small pressure anisotropy (like $G_V = 0.8G_S$, $G_V = 1.1G_S$ for the $a_0 = 0.01$ cases) under a reasonable magnetic field distribution inside QSs.

It was pointed out in Ref. [122] that to construct a hybrid star with mass heavier than $2M_\odot$ a large sound velocity square for quark matter, say larger than $1/3$, is preferred. It is known that the sound velocity square for ideal gas or for strongly coupled conformal theory can be $1/3$. However,

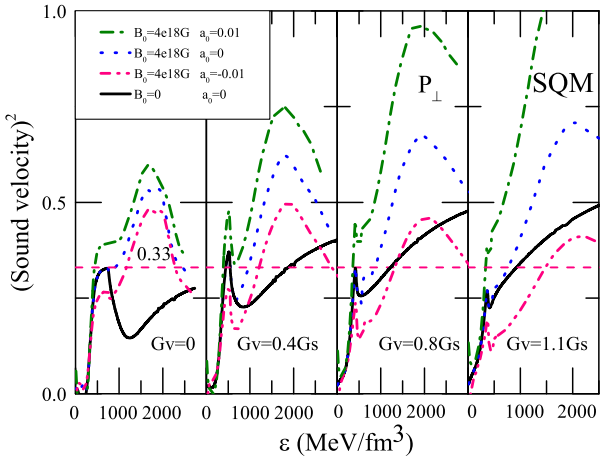

FIG. 7 (color online). The sound velocity square for transverse pressure as a function of energy density for SQM in cases $B_0 = 0$ and $B_0 = 4 \times 10^{18}$ G with $a_0 = 0, 0.01, -0.01$ and $G_V = 0$, $G_V = 0.8G_S$ and $G_V = 1.1G_S$, respectively.

for strongly interacting liquid, the sound velocity square is normally smaller than $1/3$. Therefore, it is interesting to investigate the sound velocity in our current model, and the results of sound velocity

$$c_s^2 = \frac{dp}{d\epsilon} \tag{47}$$

directly derived from equations of state in Figs. 5 and 6 are shown in Figs. 7 and 8. Because the main purpose of this work is to explore the properties of SQM under a strong magnetic field by considering the magnetized gluon contribution, we choose $B_0 = 4 \times 10^{18}$ G with $a_0 = 0$, $0.01, -0.01$ and $B_0 = 0$ with $a = 0$ by considering the vector-isoscalar interaction as $G_V = 0$, $G_V = 0.8G_S$ and $G_V = 1.1G_S$ in the following parts.

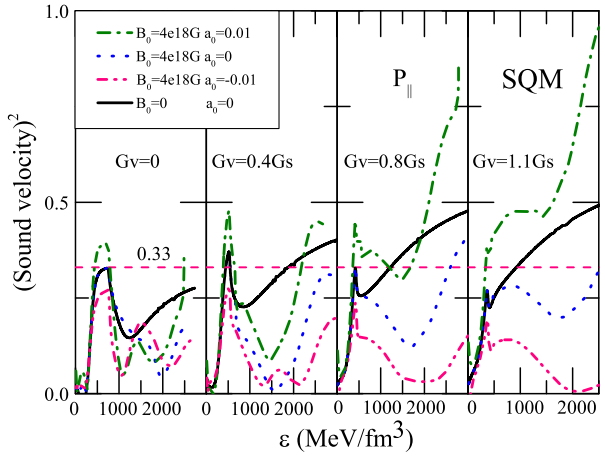

FIG. 8 (color online). The sound velocity square for longitudinal pressure as a function of energy density for SQM in cases $B_0 = 0$ and $B_0 = 4 \times 10^{18}$ G with $a_0 = 0, 0.01, -0.01$ and $G_V = 0$, $G_V = 0.8G_S$ and $G_V = 1.1G_S$, respectively.

The sound velocity square of dense quark matter for transverse pressure density in Fig. 7 in the NJL model without vector interaction ($G_V = 0$) and at $B_0 = 0$ is always less than $1/3$, which is in agreement with common sense. It is also understood that when the system is more strongly coupled, the sound velocity square is getting smaller and reaches the smallest value at the phase transition point, where the system is regarded as most strongly coupled [123].

However, it is observed that under magnetic field with magnitude of $B_0 = 4 \times 10^{18}$ G, even at $G_V = 0$, the sound velocity square for transverse pressure density case can increase to 0.6 at most. Also in the case of $B_0 = 0$, if one switches on a repulsive interaction in the vector-isoscalar channel, the sound velocity square for transverse pressure density case also increases and can become bigger than $1/3$. The stronger the G_V is, the larger sound velocity square is.

Another factor to increase the sound velocity is from the magnetized gluons. With a positive contribution from magnetized gluon pressure, and also taking into account the repulsive interaction in the vector-isoscalar channel, the sound velocity for transverse pressure case can be even larger than 1 (for the $G_V = 1.1G_S$, $B_0 = 4 \times 10^{18}$ G, and $a_0 = 0.01$ case), i.e., larger than the speed of light, which is of course not physical. So we can use the condition $c_s^2 < 1$ to constrain the EoS.

For the sound velocity square corresponding to longitudinal pressure from Fig. 8, we can find that the sound velocity square under $B_0 = 4 \times 10^{18}$ G with different G_V and a_0 are all smaller than those C_s^2 corresponding to the transverse pressure case, which is self-consisted with Figs. 5 and 6. One can also find that all the sound velocity squares corresponding to longitudinal pressure are smaller than 1.

Since we have calculated that the pressure anisotropy for SQM with the contribution from magnetized gluon pressure under the magnetic field distribution inside the QSs within $B_0 = 4 \times 10^{18}$ G, $\beta_0 = 0.003$ and $\gamma = 3$ is not big, we can approximately use the EoS from the longitudinal or transverse pressure case to construct the magnetar under a density-dependent magnetic field. We should first introduce the Tolman-Opperheimer-Volkoff (TOV) equations [124], which can give the quark star with isotropic pressure:

$$\frac{dM}{dr} = 4\pi r^2 \epsilon(r), \tag{48}$$

$$\frac{dp}{dr} = -\frac{G\epsilon(r)M(r)}{r^2}\left[1 + \frac{p(r)}{\epsilon(r)}\right] \times \left[1 + \frac{4\pi p(r) r^3}{M(r)}\right]\left[1 - \frac{2GM(r)}{r}\right]^{-1}. \tag{49}$$

We give the maximum mass of a quark star in Fig. 9 by using transverse pressure and longitudinal pressure, respectively, and we use $B_0 = 4 \times 10^{18}$ G with $a_0 = 0, 0.01, -0.01$ and $G_V = 0$, $G_V = 0.4G_S$, $G_V = 0.8G_S$, and $G_V = 1.1G_S$ for the transverse pressure case while $B_0 = 4 \times 10^{18}$ G, $a_0 = 0.01$ with $G_V = 0.8G_S$ and $G_V = 1.1G_S$ for the longitudinal pressure case. We can read the following information from Fig. 9:

(1) At $B_0 = 0$ and $G_V = 0$, the three-flavor NJL model gives the maximum mass of quark star at about $1.4M_\odot$.
(2) At $B_0 = 0$ but increasing the repulsive interaction G_V in the vector-isoscalar channel, the maximum mass of a quark star can reach $1.75M_\odot$ for $G_V = 1.1G_S$.
(3) In the case of $G_V = 0$, when one puts quark matter under the magnetic field, the maximum mass of a quark magnetar for the transverse pressure case can be as heavy as $1.65M_\odot$, and if one takes into account a positive pressure density contributed from magnetized quasigluons, the mass of a quark magnetar can reach $1.8M_\odot$.
(4) For the magnitude of $B_0 = 4 \times 10^{18}$ G, the sound velocity square for transverse pressure case reaches almost 0.9 for $G_V = 0.8G_S$ and $a_0 = 0.01$, and the magnetar mass is $2.17M_\odot$, while the maximum mass of quark star is $2.01M_\odot$ for longitudinal pressure within $G_V = 0.8G_S$ and $a_0 = 0.01$ under $B_0 = 4 \times 10^{18}$ G, which is consistent with the recently discovered large mass pulsar J0348+0432 $(2.01 \pm 0.04)M_\odot$.

To investigate the difference for the maximum mass of QSs by using longitudinal pressure and transverse pressure, we define a mass difference parameter,

$$\delta_m = \frac{M_\perp - M_{||}}{(M_\perp + M_{||})/2}, \tag{50}$$

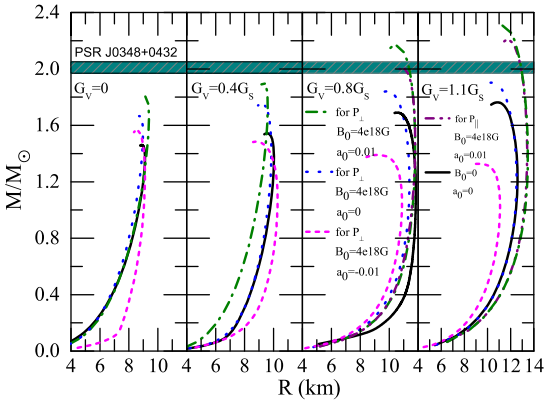

FIG. 9 (color online). Maximum mass-radius relation for the quark star for transverse and longitudinal pressure cases within $B_0 = 0$ and $B_0 = 4 \times 10^{18}$ G with $a_0 = 0, 0.01, -0.01$ and $G_V = 0$, $G_V = 0.4G_S$, $G_V = 0.8G_S$, and $G_V = 1.1G_S$, respectively.

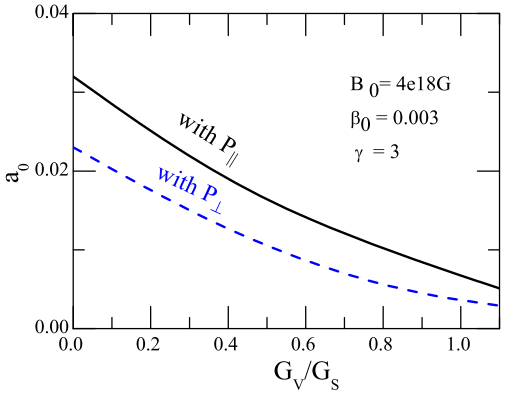

FIG. 10 (color online). The parameter region for a_0 and G_V to produce two-solar-mass QSs under $B_0 = 4 \times 10^{18}$ G and by using longitudinal pressure and transverse pressure, respectively. The parameter sets of a_0 and G_V on these two lines can produce two-solar-mass QSs.

where $M_\perp$ ($M_{||}$) represents the maximum mass of QSs with transverse (longitudinal) orientation pressure, respectively. We calculate the mass difference for the transverse and longitudinal pressure within $G_V = 0.8G_S$ and $a_0 = 0.01$ under $B_0 = 4 \times 10^{18}$ G is $\delta_m = 7.65\%$, which implies that the pressure anisotropy in this case is very small due to the tiny mass asymmetry, and this is the reason why we can use the isotropic TOV equation to calculate the properties of QSs approximately. We can also find the similar results from the $G_V = 1.1G_S$, $a_0 = 0.01$, and $B_0 = 4 \times 10^{18}$ G case that the maximum mass of the QS for transverse pressure case is $2.30M_\odot$ while $2.20M_\odot$ for the longitudinal pressure case, and the mass difference for this case is $\delta_m = 4.44\%$, which implies a smaller pressure anisotropy than the $G_V = 0.8G_S$ case. Therefore, our results indicate that we can get a stiffer EoS by considering the contributions from a density-dependent magnetic field, the repulsive interaction in the vector-isoscalar channel, and magnetized gluon pressure. Since the pressure anisotropy from a density-dependent magnetic field is not big, we can calculate the properties of QSs under a magnetic field by using isotropic TOV equation approximately, and we find the mass difference of magnetars by using that transverse and longitudinal pressure is also very small.

In Fig. 10, we show the parameter region for a_0 and G_V to produce two-solar-mass QSs under $B_0 = 4 \times 10^{18}$ G and by using longitudinal pressure and transverse pressure, respectively. The parameter sets of a_0 and G_V on these two lines can describe two-solar-mass QSs. One can see that in order to produce two-solar-mass QSs, if the repulsive vector interaction is stronger, the needed contribution from magnetized gluons is smaller, or vice versa. It is also observed that larger a_0 and G_V parameters are needed to produce two-solar-mass QSs if one uses the longitudinal pressure density. However, when the magnitude of the repulsive vector interaction increases, it is noticed that the difference between using longitudinal pressure and transverse pressure to produce two-solar-mass QSs becomes smaller because the pressure anisotropy decreases when a large contribution from the repulsive interaction in the vector-isoscalar channel is considered, which can be read from Figs. 5 and 6.

IV. CONCLUSION AND DISCUSSION

In this work, we construct quark magnetars in the framework of the SU(3) NJL model with vector interaction under a strong magnetic field.

We investigate the effect of vector-isoscalar and vector-isovector interactions on the equation of state, and it is found that the equation of state is not sensitive to the vector-isovector interaction; however, a repulsive interaction in the vector-isoscalar channel gives a stiffer equation of state for cold dense quark matter. The result is reasonable because the interaction in the vector-isovector channel shifts the isospin chemical potential, and this effect is negligible on the equation of state under β equilibrium, while the repulsive vector-isoscalar interaction shifts the chemical potential to a larger value, which makes the equation of state stiffer.

In the presence of a magnetic field, the pressure of the system is shown to be anisotropic along and perpendicular to the magnetic field direction with the former being generally larger than the latter. Gluons will be magnetized via quark loops, and we also estimate the pressure contributed from magnetized gluons. Normally, the NJL model only considers the contribution from quark degrees of freedom on the pressure, which is always underestimated. We estimate the pressure density contributed from magnetized gluons, which should be positive in order to compensate the pressure density of quasiquarks described by the NJL model. It is found that magnetized quarks and gluons also give a stiffer equation of state.

The sound velocity square is one of the fundamental properties of hot/dense matter, which measures the hardness or softness of the equation of state. It is known that hot and dense quark matter in the NJL model without vector interaction at zero magnetic field is always less than $1/3$. It is also understood that when the system is more strongly coupled the sound velocity square gets smaller and reaches the smallest value at the phase transition point, where the system is regarded as most strongly coupled. However, it is found that the sound velocity square can be larger than $1/3$ when a strong repulsive interaction is introduced, and the sound velocity square can change a lot when a strong magnetic field is added. Furthermore, the sound velocity square corresponding to the transverse pressure density case can even reach 1 when the magnetized gluon contribution is taken into account.

Since the pressure anisotropy from the density dependent magnetic field is not large, we approximately calculate the properties of QSs by using the isotropic TOV equation. We

also find the mass difference of magnetars by using the transverse and longitudinal pressure is very small. We also give the parameter region for a_0 and G_V, which can describe the two-solar-mass quark star by using longitudinal pressure and transverse pressure, respectively.

ACKNOWLEDGMENTS

We are thankful for valuable discussions with M. Alford and A. Schmitt on the sound velocity of quark matter, with J. Schaffner-Bielich and A. Sedrakian on magnetars, and with I. Shovkovy and A. Vuorinen on pressure from the magnetized gluon potential. M. H. is thankful for the hospitality of Frankfurt University, Tours University, and TU Viena, where the final stage of this work was performed. This work is supported by the National Basic Research Program of China (973 Program) under Contracts No. 2015CB856904 and No. 2013CB834405 and the NSFC under Grants No. 11275213, No. 11275125, No. 11135011, and No. 11261130311 (CRC 110 by DFG and NSFC). This work was also supported by CAS key Project No. KJCX2-EW-N01; Youth Innovation Promotion Association of CAS; the China-France collaboration project "Cai Yuanpei 2013"; the Shanghai Rising-Star Program under Grant No. 11QH1401100; the "Shu Guang" project supported by Shanghai Municipal Education Commission; and Shanghai Education Development Foundation, the Program for Professor of Special Appointment (Eastern Scholar) at Shanghai Institutions of Higher Learning, and the Science and Technology Commission of Shanghai Municipality (Grant No. 11DZ2260700).

[1] M. Baldo, G. F. Burgio, and H. J. Schulze, Phys. Rev. C **61**, 055801 (2000).
[2] E. Massot, J. Margueron, and G. Chanfray, Europhys. Lett. **97**, 39002 (2012).
[3] D. L. Whittenbury, J. D. Carroll, A. W. Thomas, K. Tsushima, and J. R. Stone, arXiv:1204.2614.
[4] G. E. Brown, V. Thorsson, K. Kubodera, and M. Rho, Phys. Lett. B **291**, 355 (1992).
[5] N. K. Glendenning and J. Schaffner-Bielich, Phys. Rev. Lett. **81**, 4564 (1998).
[6] A. Ramos, J. Schaffner-Bielich, and J. Wambach, Lect. Notes Phys. **578**, 175 (2001).
[7] E. Witten, Phys. Rev. D **30**, 272 (1984).
[8] E. Farhi and R. L. Jaffe, Phys. Rev. D **30**, 2379 (1984).
[9] M. Alford and S. Reddy, Phys. Rev. D **67**, 074024 (2003).
[10] I. Shovkovy, M. Hanauske, and M. Huang, Phys. Rev. D **67**, 103004 (2003).
[11] I. Bombaci, I. Parenti, and I. Vidaa, Astrophys. J. **614**, 314 (2004).
[12] J. Staff, R. Ouyed, and M. Bagchi, Astrophys. J. **667**, 340 (2007).
[13] M. Herzog and F. K. Röpke, Phys. Rev. D, **84**, 083002 (2011).
[14] A. Chodos, R. L. Jaffe, K. Johnson, C. B. Thorne, and V. F. Weisskopf, Phys. Rev. D **9**, 3471 (1974).
[15] J. C. Collins and M. J. Perry, Phys. Rev. Lett. **34**, 1353 (1975).
[16] G. Baym and S. A. Chin, Phys. Lett. **62B**, 241 (1976).
[17] B. Freedman and L. McLerran, Phys. Rev. D **17**, 1109 (1978).
[18] A. Drago, U. Tambini, and M. Hjorth-Jensen, Phys. Lett. B **380**, 13 (1996).
[19] N. K. Glendenning, Phys. Rev. D **46**, 1274 (1992).
[20] M. Prakash, J. R. Cooke, and J. M. Lattimer, Phys. Rev. D **52**, 661 (1995).
[21] H. Müller and B. D. Serot, Nucl. Phys. **A606**, 508 (1996).
[22] J. M. Lattimer and M. Prakash, Science **304**, 536 (2004).
[23] A. W. Steiner, M. Prakash, J. M. Lattimer, and P. J. Ellis, Phys. Rep. **411**, 325 (2005).
[24] P. Demorest, T. Pennucci, S. Ransom, M. Roberts, and J. Hessels, Nature (London) **467**, 1081 (2010).
[25] J. Antoniadis *et al.*, Science **340**, 1233232 (2013).
[26] J. M. Lattimer and M. Prakash, Phys. Rep. **442**, 109 (2007).
[27] J. M. Lattimer and M. Prakash, arXiv:1012.3208.
[28] T. Hell and W. Weise, Phys. Rev. C **90**, 045801 (2014).
[29] D. P. Menezes, M. B. Pinto, L. B. Castro, P. Costa, and C. C. Providncia, arXiv:1403.2502.
[30] V. Bernard, A. H. Blin, B. Hiller, Y. P. Ivanov, A. A. Osipov, and U. G. Meissner, Ann. Phys. (N.Y.) **249**, 499 (1996).
[31] V. Bernard, R. L. Jaffe, and U. G. Meissner, Phys. Lett. B **198**, 92 (1987).
[32] V. Bernard, R. L. Jaffe, and U. G. Meissner, Nucl. Phys. **B308**, 753 (1988).
[33] M. F. M. Lutz, S. Klimt, and W. Weise, Nucl. Phys. **A542**, 521 (1992).
[34] M. Buballa, Phys. Rep. **407**, 205 (2005).
[35] M. Hanauske, L. M. Satarov, I. N. Mishustin, H. Stoecker, and W. Greiner, Phys. Rev. D **64**, 043005 (2001).
[36] R. Huguet, J. C. Caillon, and J. Labarsouque, Nucl. Phys. **A781**, 448 (2007).
[37] R. Huguet, J. C. Caillon, and J. Labarsouque, Phys. Rev. C **75**, 048201 (2007).
[38] K. Fukushima, Phys. Rev. D **77**, 114028 (2008); **78**, 039902(E) (2008).
[39] H. Abuki, R. Gatto, and M. Ruggieri, Phys. Rev. D **80**, 074019 (2009).
[40] Z. Zhang and T. Kunihiro, Phys. Rev. D **80**, 014015 (2009).
[41] N. M. Bratovic, T. Hatsuda, and W. Weise, Phys. Lett. B **719**, 131 (2013).
[42] G. Y. Shao, M. Colonna, M. Di Toro, Y. X. Liu, and B. Liu, Phys. Rev. D **87**, 096012 (2013).

[43] T. Klahn, R. Lastowiecki, and D. B. Blaschke, Phys. Rev. D **88**, 085001 (2013).
[44] J. Xu, T. Song, C. M. Ko, and F. Li, Phys. Rev. Lett. **112**, 012301 (2014).
[45] J. Steinheimer and S. Schramm, Phys. Lett. B **696**, 257 (2011).
[46] J. Steinheimer and S. Schramm, Phys. Lett. B **736**, 241 (2014).
[47] D. P. Menezes, M. Benghi Pinto, S. S. Avancini, and C. Providencia, Phys. Rev. C **80**, 065805 (2009).
[48] V. Skokov, A. Y. Illarionov, and V. Toneev, Int. J. Mod. Phys. A **24**, 5925 (2009).
[49] W. T. Deng and X. G. Huang, Phys. Rev. C **85**, 044907 (2012).
[50] B. I. Abelev *et al.* (STAR Collaboration), Phys. Rev. C **81**, 054908 (2010).
[51] B. Abelev *et al.* (ALICE Collaboration), Phys. Rev. Lett. **110**, 012301 (2013).
[52] D. Kharzeev and A. Zhitnitsky, Nucl. Phys. **A797**, 67 (2007).
[53] D. E. Kharzeev, L. D. McLerran, and H. J. Warringa, Nucl. Phys. **A803**, 227 (2008).
[54] K. Fukushima, D. E. Kharzeev, and H. J. Warringa, Phys. Rev. D **78**, 074033 (2008).
[55] S. P. Klevansky and R. H. Lemmer, Phys. Rev. D **39**, 3478 (1989).
[56] K. G. Klimenko, Theor. Math. Phys. **89**, 1161 (1991).
[57] V. P. Gusynin, V. A. Miransky, and I. A. Shovkovy, Nucl. Phys. **B462**, 249 (1996); **B563**, 361 (1999).
[58] G. S. Bali, F. Bruckmann, G. Endrodi, Z. Fodor, S. D. Katz, S. Krieg, A. Schafer, and K. K. Szabo, J. High Energy Phys. 02 (2012) 044.
[59] G. S. Bali, F. Bruckmann, G. Endrodi, Z. Fodor, S. D. Katz, and A. Schafer, Phys. Rev. D **86**, 071502 (2012).
[60] G. S. Bali, F. Bruckmann, G. Endrodi, F. Gruber, and A. Schaefer, J. High Energy Phys. 04 (2013) 130.
[61] J. Chao, P. Chu, and M. Huang, Phys. Rev. D **88**, 054009 (2013).
[62] L. Yu, H. Liu, and M. Huang, Phys. Rev. D **90**, 074009 (2014).
[63] M. N. Chernodub, Phys. Rev. D **82**, 085011 (2010).
[64] M. N. Chernodub, Phys. Rev. Lett. **106**, 142003 (2011).
[65] M. Frasca, J. High Energy Phys. 11 (2013) 099.
[66] H. Liu, L. Yu, and M. Huang, arXiv:1408.1318.
[67] R. Mallick, S. Schramm, V. Dexheimer, and A. Bhattacharyya, arXiv:1408.0139.
[68] A. Lyne and F. Graham-Smith, *Pulsar Astronomy* (Cambridge University Press, Cambridge, England, 2005).
[69] C. Woltjer, Astrophys. J. **140**, 1309 (1964).
[70] T. A. Mihara *et al.*, Nature (London) **346**, 250 (1990).
[71] G. Chanmugam, Annu. Rev. Astron. Astrophys. **30**, 143 (1992).
[72] C. Thompson and R. C. Duncan, Astrophys. J. **473**, 322 (1996).
[73] A. I. Ibrahim, S. Safi-Harb, J. H. Swank, W. Parke, and S. Zane, Astrophys. J. **574**, L51 (2002).
[74] R. C. Duncan and C. Thompson Astrophys. J. **392**, L9 (1992).
[75] D. Lai and S. L. Shapiro, Astrophys. J. **383**, 745 (1991).
[76] E. J. Ferrer, V. de la Incera, J. P. Keith, I. Portillo, and P. L. Springsteen, Phys. Rev. C **82**, 065802 (2010); E. J. Ferrer and V. de la Incera, Lect. Notes Phys. **871**, 399 (2013).
[77] A. A. Isayev and J. Yang, Phys. Rev. C **84**, 065802 (2011).
[78] A. A. Isayev and J. Yang, Phys. Lett. B **707**, 163 (2012).
[79] A. A. Isayev and J. Yang, J. Phys. G **40**, 035105 (2013).
[80] D. Bandyopadhyay, S. Chakrabarty, and S. Pal, Phys. Rev. Lett. **79**, 2176 (1997).
[81] D. Bandyopadhyay, S. Pal, and S. Chakrabarty, J. Phys. G **24**, 1647 (1998).
[82] D. P. Menezes, M. Benghi Pinto, S. S. Avancini, A. Perez Martinez, and C. Providencia, Phys. Rev. C **79**, 035807 (2009).
[83] R. Casali, L. B. Castro, and D. P. Menezes, Phys. Rev. C **89**, 015805 (2014).
[84] M. Strickland, V. Dexheimer, and D. P. Menezes, Phys. Rev. D **86**, 125032 (2012).
[85] M. Sinha, X. G. Huang, and A. Sedrakian, Phys. Rev. D **88**, 025008 (2013).
[86] R. Z. Denke and M. B. Pinto, Phys. Rev. D **88**, 056008 (2013).
[87] V. Dexheimer, R. Negreiros, and S. Schramm, Eur. Phys. J. A **48**, 189 (2012).
[88] P. C. Chu, L. W. Chen, and X. Wang, Phys. Rev. D **90**, 063013 (2014).
[89] P. Zhuang, J. Hufner, and S. P. Klevansky, Nucl. Phys. **A576**, 525 (1994).
[90] G. Boyd, J. Engels, F. Karsch, E. Laermann, C. Legeland, M. Lutgemeier, and B. Petersson, Nucl. Phys. **B469**, 419 (1996).
[91] K. Fukushima, Phys. Lett. B **591**, 277 (2004).
[92] C. Ratti, M. A. Thaler, and W. Weise, Phys. Rev. D **73**, 014019 (2006).
[93] V. A. Dexheimer and S. Schramm, Phys. Rev. C **81**, 045201 (2010).
[94] V. A. Dexheimer and S. Schramm, Nucl. Phys. B, Proc. Suppl. **199**, 319 (2010).
[95] D. Blaschke, J. Berdermann, and R. Lastowiecki, Prog. Theor. Phys. Suppl. **186**, 81 (2010).
[96] G. Y. Shao, Phys. Lett. B **704**, 343 (2011).
[97] O. Lourenco, M. Dutra, T. Frederico, A. Delfino, and M. Malheiro, Phys. Rev. D **85**, 097504 (2012).
[98] R. C. Duncan, arXiv:astro-ph/0002442.
[99] C. Sasaki, B. Friman, and K. Redlich, Phys. Rev. D **75**, 054026 (2007).
[100] L. Levkova and C. DeTar, Phys. Rev. Lett. **112**, 012002 (2014).
[101] B. A. Freedman and L. D. McLerran, Phys. Rev. D **16**, 1169 (1977).
[102] V. Baluni, Phys. Rev. D **17**, 2092 (1978).
[103] J. P. Blaizot, E. Iancu, and A. Rebhan, Phys. Rev. D **63**, 065003 (2001).
[104] E. S. Fraga, R. D. Pisarski, and J. Schaffner-Bielich, Phys. Rev. D **63**, 121702 (2001).
[105] E. S. Fraga, R. D. Pisarski, and J. Schaffner-Bielich, Nucl. Phys. **A702**, 217 (2002).
[106] J. O. Andersen and M. Strickland, Phys. Rev. D **66**, 105001 (2002).
[107] A. Vuorinen, Phys. Rev. D **68**, 054017 (2003).

[108] E. S. Fraga and P. Romatschke, Phys. Rev. D **71**, 105014 (2005).
[109] A. Ipp, K. Kajantie, A. Rebhan, and A. Vuorinen, Phys. Rev. D **74**, 045016 (2006).
[110] A. Kurkela, P. Romatschke, and A. Vuorinen, Phys. Rev. D **81**, 105021 (2010).
[111] A. Kurkela, E. S. Fraga, J. Schaffner-Bielich, and A. Vuorinen, Astrophys. J. **789**, 127 (2014).
[112] N. Haque, A. Bandyopadhyay, J. O. Andersen, M. G. Mustafa, M. Strickland, and N. Su, J. High Energy Phys. 05 (2014) 027.
[113] S. Mogliacci, arXiv:1407.2191.
[114] V. A. Miransky and I. A. Shovkovy, Phys. Rev. D **66**, 045006 (2002).
[115] E. Megias, E. Ruiz Arriola, and L. L. Salcedo, J. High Energy Phys. 01 (2006) 073.
[116] F. Xu and M. Huang, Chin. Phys. C **37**, 014103 (2013).
[117] N. M. Hugenholtz and L. van Hove, Physica (Amsterdam) **24**, 363 (1958).
[118] D. P. Menezes, M. Pinto, S. Benghi, S. Avancini, A. Martinez, and C. Providência, Phys. Rev. C, **79**, 035807 (2009).
[119] D. P. Menezes, M. Pinto, S. Benghi, S. Avancini, and C. Providência, Phys. Rev. C **80**, 065805 (2009).
[120] C. Y. Ryu, K. S. Kim, and Myung-Ki Cheoun, Phys. Rev. C, **82**, 025804 (2010).
[121] C. Y. Ryu, Myung-Ki Cheoun, T. Kajino, T. Maruyama, and G. J. Mathews, Astropart. Phys. **38**, 25 (2012).
[122] M. G. Alford, S. Han, and M. Prakash, Phys. Rev. D **88**, 083013 (2013).
[123] H. Mao, J. Jin, and M. Huang, J. Phys. G **37**, 035001 (2010).
[124] J. R. Oppenheimer and G. M. Volkoff, Phys. Rev. **55**. 374 (1939).